Electromagnetic and Thermal Analysis/Design of an Induction Motor for Electric Vehicles

Cenk Ulu
Yıldız Technical University
Department of Mechatronics Engineering
Istanbul, Turkey
e-mail: cenkulu@yildiz.edu.tr

Oğuz Korman and Güven Kömürgöz
Istanbul Technical University
Department of Electrical Engineering
Istanbul, Turkey
Email: oguz.korman@gmail.com, komurgoz@itu.edu.tr

***Abstract*—Induction machines are the most commonly used electrical machines in applications, since they are durable, easy to manufacture and control. Additionally, they require less maintenance and response different loads. In this study, the design of 115kW (continuous 85kW) squirrel cage induction motor is presented for electric vehicle applications. Main design constraints and performance criteria of the motor are determined, and the computer-aided design is performed depending on these values. In the design procedure, initially, an analytical design of the electric vehicle motor is performed depending on specified design criteria. Then, the analytical design is verified by using finite element analyses. Depending on the obtained results in electro-magnetic analyses, the squirrel cage induction motor for electric vehicle is modified in order to improve the obtained performance further. The electromagnetic and thermal analyses of the designed motor are performed by using Maxwell® and ANSYS software programs, respectively. The insulation class of the designed motor is determined by considering the maximum allowable temperature criterion. The analyses results show that the designed motor satisfies design constraints and performance criteria.**

***Index Terms*—induction motor, electric vehicle, thermal analysis, electromagnetic analysis**

I. Introduction

Popularity of the electric vehicles (EVs) has continuously increased worldwide depending on the decreasing petrol sources and increasing emissions. Therefore, many vehicle manufacturers have launched various commercial electric vehicles such as Toyota RAV4 EV, Chevrolet Volt, Tesla Model S and Renault Twizy [1, 2].

Electric powered vehicles mainly consist of four subsystems: Battery, traction motor, motor driver and control units. The battery unit supplies the required power to both the traction system and the electrical equipment of the vehicle. It is the duty of the battery management system to check the battery level and the temperature so that they do not exceed any critical levels. In the traction system, an electric motor is used which is generally a brushless permanent magnet motor [3, 4], a squirrel cage induction motor [5, 6] or a switch reluctance motor [7, 8]. The motor driver is used for variable speed/torque control of the motor as well as regenerative breaking. The control unit collects all available data from the other subsystems/components, and performs the high-level control of the vehicle.

Asynchronous motors are widely used in the industry for their low cost and robustness. Industrial asynchronous motors are generally used without driver and usually do not operate at extreme working cycles. These motors are designed with respect to constant voltage and constant frequency values depending on the grid voltage and frequency values. In literature, there are many analytical and experimental data and tables for the design of these types of asynchronous motors. In the design process, these results help the designer to determine suitable values of design parameters such as pole number, slot type, airgap value, current and flux density values. On the other hand, motors with driver operate at variable frequency, voltage and power values as it is in the electric vehicle applications. Therefore, the most of the data and tables (such as stator-rotor slot combination) used in the design procedure of industrial asynchronous motors are not valid anymore for the design of variable frequency asynchronous motors. In the case of electric vehicle applications, an electric motor must fit the driving pattern by satisfying the different speed and torque characteristics. This necessity leads to special considerations in the motor design for electrical vehicles.

Manuscript received February 11, 2018; revised August 28, 2018.

doi: 10.18178/ijmerr.7.6.617-623

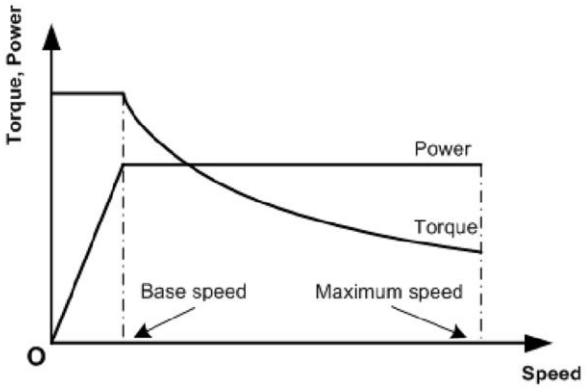

Figure 1. Power and torque characteristics of electric motor

In Fig. 1, the torque and power characteristics of an electric motor with driver are given [9]. The operating region under the base frequency is named as the constant torque region. In this region, the maximum torque value that is needed for acceleration of the electric vehicle can be provided constantly for different speeds by controlling voltage and frequency. The region between the base and maximum frequencies is named as the constant power region. Since the maximum voltage value obtained from the driver is limited depending on the capacity of the battery pack, the power of the motor becomes constant above the base frequency. Therefore, the torque obtained from the motor decreases in the constant power region when the motor speed increases.

In this study, 115kW (continuous 85kW) squirrel cage induction motor is designed and the results of electromagnetic and thermal analyses are given.

II. Induction Motor Design

A. Factors that Affect Electrical Machine Design

In the electrical machine design, economical factors, limits related to motor materials, requirements related to standards, and other special factors that have effects on the design are taken into consideration [10].

In industry, the cost of an electrical machine has generally great importance. Technical and economical limits related with materials such as thickness and magnetic saturation values of steel laminations, the size and type of conductor and dielectric materials directly affect the size and performance of electrical machines by determining the maximum flux density values, losses, efficiency and the weight.

The electrical machine should be designed, manufactured and tested depending on international standards such as IEEE, IEC, NEMA [11-13]. On the other hand, there may be special conditions for the electrical machine. For example, the electrical machine can be used in the environment having extreme temperature conditions. In this case, these requirements must be considered specially in the design process.

B. Design Steps

Before starting the design procedure of an electrical machine, design criteria such as power, phase number, supply voltage, frequency, desired efficiency, power factor, conductor current density, air gap flux density are specified. Then, the design process is initiated, and systematic revisions are performed by modifying design parameters on the motor model until design criteria are met.

The design steps of an electrical machine can be given as follows [10].

- Electrical design: Depending on given electrical design criteria, stator and rotor dimensions, slot numbers, winding type, coil dimensions and numbers, coil factors, motor connection type, etc., of electrical machine are determined.
- Magnetic design*:* Depending on given design criteria, lamination saturation flux density and airgap flux density are determined. Depending on these values, stator and rotor teeth and yokes are designed.
- Insulation design*:* The motor insulation design is performed to provide electrical safety by considering the motor operating temperature and the winding voltage.
- Thermal design*:* Since the coil resistance increases when the temperature increases, thermal design has important effect on the motor efficiency. Therefore, thermal design is performed to keep the motor at its desired operation temperature. In the thermal design, cooling type, cooling flow rate, ventilation ducts, etc., are determined.
- Mechanical design: In mechanical design of the electrical machine, shaft design, bearing design, end bracket design and motor frame design are performed by considering critical working speed, noise and vibration of the electrical machine, tensile forces acting on shaft, moment of inertia, etc.

C. Special Considerations in the Design of Asynchronous Motors with Driver

In the design procedure of the electric motor for EVs, initially, it is needed to determine the base frequency w_b where the nominal power value is desired to be obtained. In this way, the operating frequency range is determined depending on the desired maximum operating frequency w_{max}. The base operating frequency depends on the determined nominal speed and pole number of the motor. When the pole number is determined, it is important to consider that the maximum operating frequency should not be considerably high. Because, higher maximum frequencies result in higher iron and eddy current losses in the electrical machine. Additionally, the maximum operating speed is directly related with the breakdown torque value of the electrical machine. In order to provide desired maximum operating speed, the breakdown torque value of the motor must be high. Therefore, the leakage inductances in the electrical machine design must be decreased as far as possible.

Second, the voltage range of the battery pack of the EV is considered in the design procedure. The design of the motor can be performed with respect to the minimum voltage value of the battery pack in order the motor to provide desired torque value in even the worst case. On the other hand, increasing motor voltage directly affects the flux density values in the lamination and airgap. Therefore, in the design, it should be considered that, the flux density values should be under the magnetic saturation value of the lamination material at the maximum operating voltage.

Finally, the maximum power requirement of the EV is an important factor for the electrical and thermal design of the motor. The value and period of the maximum power depend on the current density limit of the motor windings. When the motor is operated above its continuous (nominal) power, the motor current increases. This results in rapid increase at the winding temperature. The duration of the maximum power operation directly depends on the thermal performance of the motor. Therefore, the designed motor should tolerate the maximum power demand in reasonable duration.

D. Design Constraints and Criteria

Electric motor is one of the subsystems of the EV such as battery pack and main control unit. Therefore, there are various constraints in the design procedure depending on the specifications of the other subsystems of the EV. The design constraints and criteria of the electric motor are given in Table I.

TABLE I. DESIGN CRITERIA AND CONSTRAINTS

Motor phase voltage	440VAC
Motor nominal speed	2250 rpm
Motor maximum speed	>6000 rpm
Motor nominal torque	360 Nm (85kW)
Motor maximum torque	476 Nm (115kW)
Efficiency	%92
Motor cooling type	Totally enclosed
Motor operating temperature	135 ℃
Available volume for motor in EV	450x450x400mm

E. Choice of Pole Number/Operating Frequency

Before starting the motor design, pole number/operating frequency of the motor must be determined depending on the values given in Table I. The frequency of a motor is calculated as follows

$$f_1 = \frac{np}{60} \tag{1}$$

where n and p denote speed and single pole number of the motor.

By using (1), the nominal and maximum operating frequencies of the motor are calculated as given in Table II with respect to the different pole number values.

TABLE II. CHANGE OF MOTOR OPERATING FREQUENCY VALUES WITH RESPECT TO POLE NUMBER

Pole Number ($2p_1$)	Nominal Operating Frequency (Hz)	Maximum Operating Frequency (Hz)
2	37.5	108
4	75	217
6	112.5	325
8	150	433

When operating frequency of the motor increases, losses depending on the motor frequency such as iron and eddy current losses also increase. Considering this point and also desired power requirements, the pole number of the motor is chosen as $2p_1 = 4$.

F. Electrical and Magnetic Design

Before starting the electrical machine design, electrical and magnetic limitations must be determined in addition to performance criteria and constraints given in Table I. The maximum design parameter values are determined as given in Table III.

TABLE III. MAXIMUM DESIGN PARAMETER VALUES

Parameter	Max. Value
Stator current density	8 A/mm^2
Rotor bar current density	6 A/mm^2
Rotor ring current density	4 A/mm^2
Lamination flux density	2.2 T

Considering iron losses, the thickness of lamination material is chosen as 0.35mm. Its magnetic saturation value is 2.3T and its iron loss is 2.5 W/kg (at 1.5 Tesla/50 Hz). The rotor cage is die-cast aluminum. Analytical and magnetic analyses are performed and the motor design is improved with respect to analyses results. Ansoft RMxprt and Maxwell 2D software packages are used in the analytical and magnetic analyses of the motor, respectively.

Main dimensions of the motor are determined depending on the values given in Table I by using the output coefficient design method [14]. Stator and rotor design of the motor is performed depending on the specified design values. After systematic analyses, the stator and rotor slot combination is determined as 48/54 to reduce unbalanced rotor forces and harmonics. Additionally, since the breaking torque has to be high enough to enable required maximum speed, leakage inductances are diminished sufficiently.

The lamination geometries of the designed motor and their parameter values are given in Fig. 2 and Table IV, respectively.

TABLE IV. PARAMETER VALUES OF LAMINATION GEOMETRIES

Parameter	Stator	Rotor
Slot number	48	58
Outer diameter	320mm	209
Inner diameter	210mm	60mm
Length	225 mm	

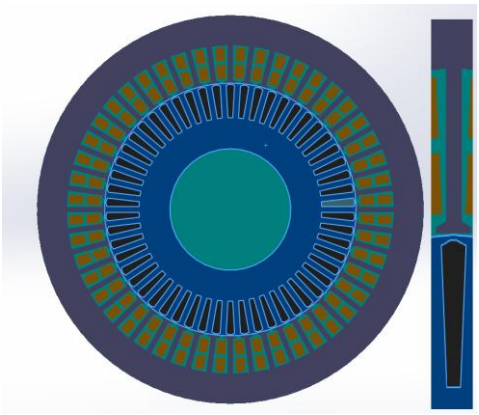

Figure 2. Stator and rotor lamination geometries

III. Thermal Design

Thermal considerations of electric motors hold great importance since all the motor materials are sensitive to heat. Resistivity of the copper increases with increasing temperature and this leads to decrease of the motor torque which is unfavorable especially in electric vehicle applications.

Heat is transferred in three ways: conduction, convection and radiation. Conduction occurs between in-touch bodies whereas convection is the transfer of heat by means of a fluid. Radiation is the heat transfer between two surfaces where a fluid is not required. Generally, radiation is not taken into consideration in electric motors as its effect is relatively small. Conduction is mostly seen in the rotor, where rotor bars heat the rotor laminations.

For isotropic media, the steady-state heat transfer governing equations and its boundary conditions can be given as below:

$$\nabla\left(-k\nabla T\right)=Q \tag{2}$$

$$k\frac{\partial T}{\partial n}\bigg|_{s}=0 \tag{3}$$

$$k\frac{\partial T}{\partial n}\bigg|_{s}=-h\left(T-T_{f}\right) \tag{4}$$

where, k [W/mK] is the thermal conductivity, T [K] is the temperature, and Q [W/m^3] is the heat source, n is the unit normal vector, h [W/(m^{2}K)] is the heat transfer coefficient, T_f [K] is the fluid temperature (temperature of the cooling agent). The heat sources leading to the temperature rising of the motor come from all losses of the motor. These losses consist of losses of the stator winding, rotor bar losses, iron-core losses, mechanical losses and additional losses.

Convection is the most important heat transfer type in an electric motor because it helps the motor to cool. In this paper, convection in the air gap is studied and results are used in the heat transfer analysis since the convection in the air gap is quite important. Fluid in the air gap, generally air, removes the heat generated from the stator and rotor. Forces occurring from the rotating rotor forces the fluid to tangential movement and therefore toroidal vortices are induced [15]. This movement is known as Taylor vortex flow and described by Taylor number as:

$$Ta_m=\frac{\Omega_a r_m^{0.5}\left(b-a\right)^{1.5}}{\nu} \tag{5}$$

Low Taylor numbers indicate that heat transfer is closer to the conduction rather than the convection. When the number is between 1700 and 10^4, vortices happen with laminar flow and (7) is used for Nusselt number calculation. For Taylor numbers higher than 10^4, flow is turbulent and Nusselt number is modeled as in (8). (6) is critical speed for determination of vortices.

$$\Omega_{cr}=\frac{41.19\nu}{r_m^{0.5}\left(b-a\right)^{1.5}} \tag{6}$$

$$Nu=0.128Ta_m^{\,0.367}\qquad 1700<Ta_m<10^4 \tag{7}$$

$$Nu=0.409Ta_m^{\,0.241}\qquad 10^4<Ta_m<10^7 \tag{8}$$

$$h=\frac{Nuk}{D_h} \tag{9}$$

where, Ω_a is the motor speed, ν is the kinematic viscosity, r_m is the rotor radius, b is the airgap outer diameter, a is the airgap inner diameter, Ta_m is Taylor's number, Nu is Nusselt number, and D_h is the air gap length.

It is shown that h-convection coefficient obtained from the numerical analysis shows very good agreements to values obtained from analytical [16]. CFD analysis is performed to verify the analytically calculated values of h.

IV. Analyses Results

A. Electromagnetic Analyses

Electrical and magnetic analyses of the designed motor are performed on Maxwell software. The results are shown for the maximum power condition in order to investigate the worst scenario where the motor operates at its extreme operating point.

For the maximum power-operating mode, calculated winding currents and corresponding flux lines distribution are given in Fig. 3 and Fig. 4, respectively.

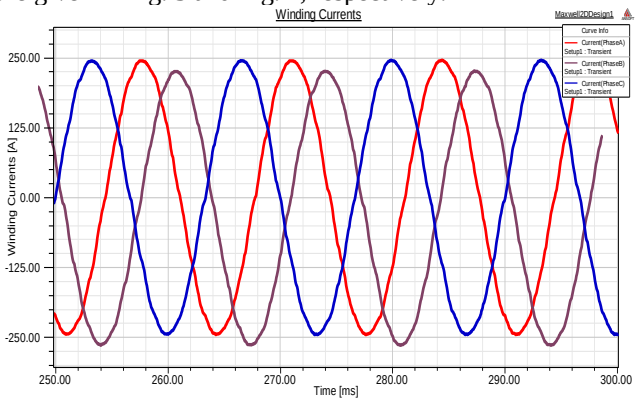

Figure 3. Phase currents in maximum power operating mode

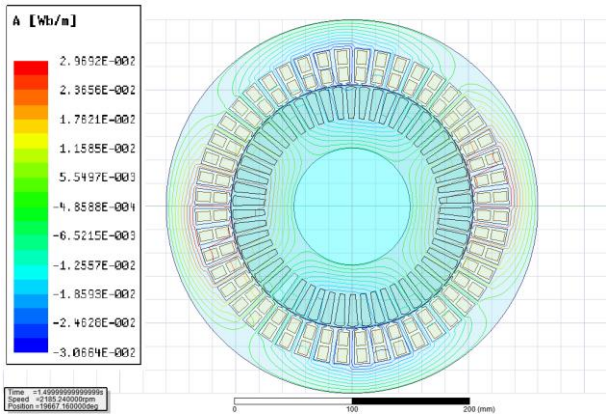

Figure 4. Flux lines distribution

As it is seen from Fig. 4, flux lines are distributed properly and desired winding poles are obtained. The magnetic flux density distribution of the motor lamination are given in Fig. 5.

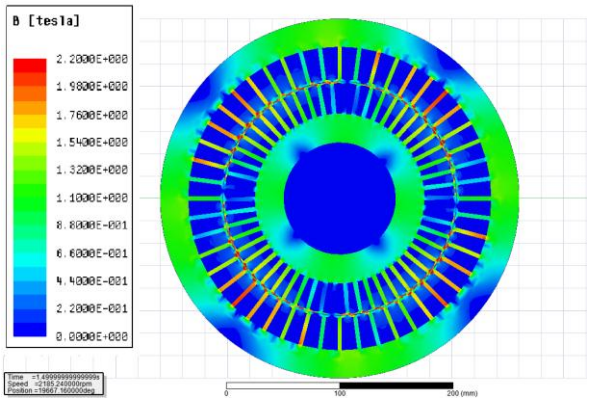

Figure 5. Flux density distribution

As it is seen from Fig. 5, flux density values are mostly less than 2T. Although there are some narrow regions such as slot openings where flux density values are greater than 2T, the maximum flux density value is less than 2.3T which is the magnetic saturation value of the motor lamination material.

The input-output power and torque computations of the designed motor are given in Fig. 6 and Fig. 7, respectively.

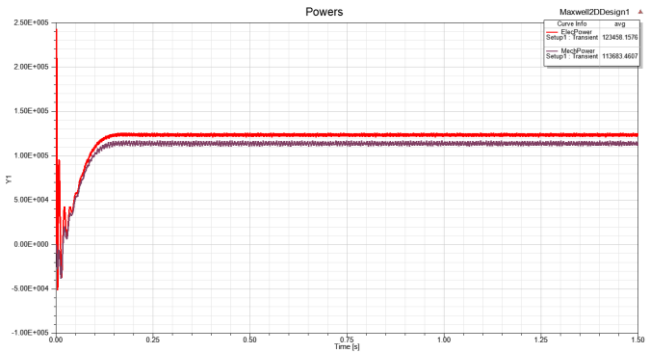

Figure 6. Electrical and mechanical power of the motor

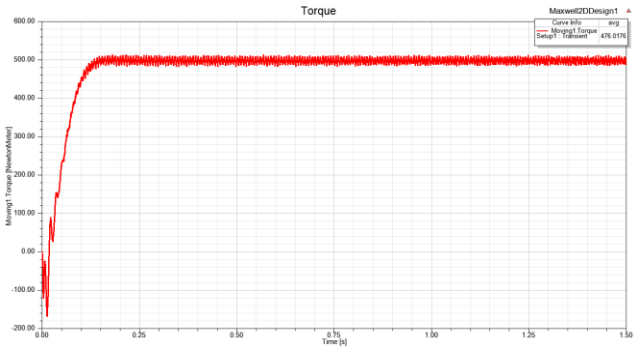

Figure 7. FEA torque computation

As it is seen from Fig. 6 and Fig. 7, the motor efficiency is approximately 92% and the torque value is 490Nm. Torque ripples are under the acceptable ranges.

Finally, analyses results of the designed motor are given in Table V.

TABLE V. ELECTROMAGNETIC ANALYSES RESULTS

Parameter	Value
Mechanical output power	115055 W
Shaft torque	490 Nm
Electrical input power	124169 W
Power factor	0.91
Efficiency	92.66%
Stator current density	7.56 A/mm^2
Rotor bar current density	5.40 A/mm^2
Rotor ring current density	3.60 A/mm^2
Nominal operating frequency	75 Hz
Nominal operating speed	2250 rpm

As it is seen from Table V, desired power, torque and efficiency criteria are satisfied. Additionally, obtained current density values are less than their specified limits given in design criteria. Thus, the designed motor satisfies all electrical and magnetic design criteria.

Motor is controlled by using the flux-weakening control method. In this case, the output power and torque curves with respect to the motor speed are given in Fig. 8 and Fig. 9, respectively, for the cases of nominal-maximum power values.

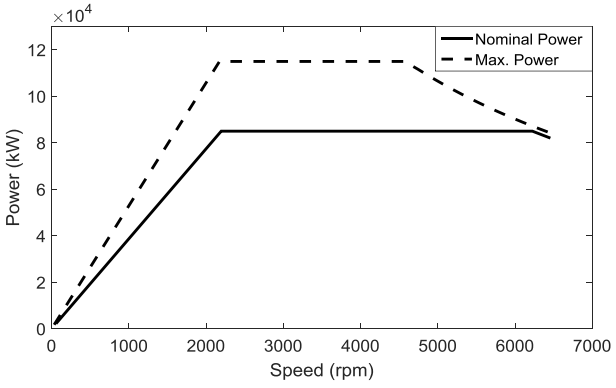

Figure 8. Output power with flux-weakening control

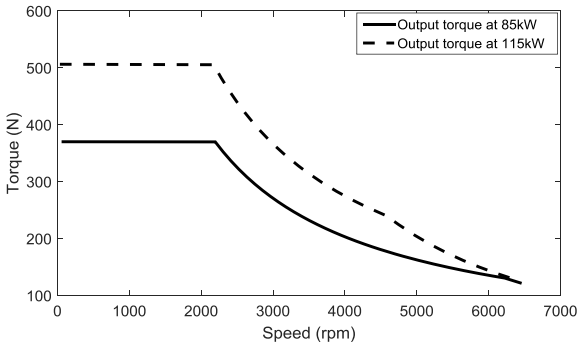

Figure 9. Output Torque with flux-weakening control

As it is seen from Fig. 8 and Fig. 9, the maximum operating speed of the designed motor in constant power region is approximately 6300 rpm and thus, the design criterion of the maximum operating speed is satisfied.

B. Thermal Analysis

Thermal analyses are done in the steady state condition which means that as if the motor has operated for a certain amount of time until a temperature change does not occur. Temperature distribution of an electric motor gives very valuable information to the designer. High temperature warns the designer to decrease the losses, change the effective cooling type, adjust the fins and frame, propose a new cooling type or optimize the motor. Force convection over the motor will further increase the heat dissipation leading to decrease in temperature. Electromagnetic analysis results show the losses in the machine. These results are used as an input to the thermal analysis software. Core and ohmic losses are behaved as an internal heat generation. Convective heat transfer coefficients are calculated by using (5) to (9).

Dimensions of the designed induction motor are given in Table IV. The motor is insulated as H class insulation. By using these dimensional parameter values, the air gap convection value is found to be 70 W/m^{2}K.

The heat sources leading to the temperature rising of the motor come from all losses of the motor. Winding losses of the stator, rotor bar losses, iron-core losses, mechanical losses, and additional losses are applied as heat sources in analyses. Boundary conditions, given in (3) and (4), are then applied to the boundary, and the temperature field distribution of the motor is obtained as shown in Fig. 10.

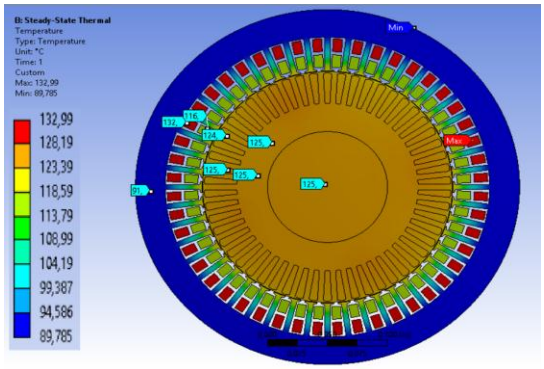

Figure 10. Temperature distribution of the motor at 115 kW

As shown in Fig. 10, the maximum temperature is found in the stator winding and rotor bars. The temperature difference between the rotor core and the rotor bar is small, and the highest temperature appears in the stator upper winding. The heat is mainly conducted to the stator through the air-gap, and then taken away. The heat exchange occurs between the stator and the rotor over the air gap. It is also seen that the temperature of the stator upper winding is higher than that of the lower winding in the slot, and the temperature of the stator core yoke is lower. Fan on the shaft to force convection over the motor increases the heat dissipation and decreases the temperature on lower windings sections.

The maximum winding temperature is seen as 133 ℃. It is important that the radiation does not taken into account in thermal analyses, only natural convection is investigated. If outer frame is as well designed, more heat is going to be extracted from the surface of the stator by convection and what is more, considering the radiation in calculations would increase the extraction.

V. Results and Discussion

In this study, a squirrel cage induction motor is designed for electric vehicle traction applications. Relevant magnetic and thermal analyses are performed and their results are presented. Analyses results show that the designed motor satisfies the desired electromagnetic and thermal requirements. In the design of the electric motor, Maxwell® and ANSYS software programs are used for magnetic analyses and thermal analyses, respectively.

The thermal analyses are performed for steady state condition when the motor operates at its maximum power. For the maximum overload condition, it is seen that the temperatures are enough when the operation cycle is considered. The motor insulation class is chosen as H class in order to withstand the maximum allowable temperature. The obtained temperature rise is lower than the allowable temperature rise of insulation. This means that the hot spot temperature will decrease and the motor life will be extended. To obtain full temperature distribution, it is necessary to calculate end winding temperatures. For this, 3D analysis should be realized in the future.

References

[1] T. Elwert, D. Goldmann, F. Römer, M. Buchert, C. Merz, D. Schueler, and J. Sutter, "Current developments and challenges in the recycling of key components of (Hybrid) electric vehicles," *Recycling*, vol. 1, pp. 25-60, 2016

[2] A. K. Balaji, T. Raj, F. Patel, and P. K. Soori, "Intelligent inductive power transfer systems for electric vehicles," in *Proc. 2016 IEEE International Conference on Emerging Technologies and Innovative Business Practices for the Transformation of Societies (EmergiTech)*, Balaclava, 2016, pp. 1-4.

[3] J. Nerg, M. Rilla, V. Ruuskanen, J. Pyrhönen, and S. Ruotsalainen, "Design of direct-driven permanent magnet synchronous motors for an electric sports car," *2012 XXth International Conference on Electrical Machines*, Marseille, 2012, pp. 177-182.

[4] Y. K. Chin and J. Soulard, "A permanent magnet synchronous motor for traction applications of electric vehicles," *IEEE International*

Electric Machines and Drives Conference, IEMDC'03, 2003, pp. 1035-1041.

[5] B. Kim *et al*., "Development of 50kW traction induction motor for electric vehicle (EV)," *IEEE Vehicle Power and Propulsion Conference (VPPC)*, 2012, pp 142-147.

[6] G. Pellegrino, A. Vagati, B. Boazzo, and P. Guglielmi, "Comparison of induction and PM synchronous motor drives for EV application including design examples," in *IEEE Transactions on Industry Applications*, vol. 48, no. 6, pp. 2322-2332, Nov.-Dec. 2012.

[7] C. P. Riley *et al*., "Simulation based design of reluctance motors for traction applications in hybrid and electric vehicles," *7th IET International Conference on Power Electronics, Machines and Drives (PEMD 2014)*, Manchester, 2014, pp. 1-6.

[8] A. G. Jack, B. C. Mecrow, and C. Weiner, "Switched reluctance and permanent magnet motors suitable for vehicle drives-a comparison," *Electric Machines and Drives, 1999. International Conference IEMD '99*, Seattle, WA, 1999, pp. 505-507.

[9] M. Ehsani, Yimin Gao, and S. Gay, "Characterization of electric motor drives for traction applications," Industrial Electronics Society, 2003. IECON '03. The 29th Annual Conference of the IEEE, 2003, pp. 891-896 vol.1.

[10] T. A. Lipo, Introduction to AC machine design**,** Wisconsin Power Electronics Research Center, 2004

[11] IEEE Std 112-2004, IEEE Standard Test Procedure for Polyphase Induction Motors and Generators

[12] IEC 60034- 1:2017 Rotating electrical machines - Part 1: Rating and performance

[13] NEMA MG 1-2016 Motors and Generators

[14] I. Boldea and S. A. Nasar, *The Induction Machines Design Handbook*, Taylor & Francis Group, 2010

[15] D. A. Howey, P. R. N. Childs, and A. S. Holmes, "Air-gap convection in Rotating electrical machines," in *IEEE Transactions on Industrial Electronics*, vol. 59, no. 3, pp. 1367-1375, March 2012.

[16] M. Jaaskelainen, "Determinaiton of coefficients of thermal convection in a high-speed electrical machine," Master's Thesis. Helsinky University of Technology.

Cenk Ulu received the B.Sc. degree in electrical engineering from Yıldız Technical University, Istanbul, Turkey, in 2004 and the M.S. and the Ph.D degrees in control engineering from Istanbul Technical University, Istanbul, Turkey, in 2006 and 2013, respectively. He is currently an Associate Professor in the Department of Mechatronics Engineering at Yıldız Technical University, Turkey. His current research interests include fuzzy modeling and control, type-2 fuzzy logic systems, intelligent control systems and electrical machine design.

Oğuz Korman completed his BS (2015) and currently studying MS in electrical engineering in Istanbul Technical University. His interests include design of PM motors, FE analysis and analytical techniques. He is working in Akım Metal R&D Department in electromagnetic design and analysis.

Güven Komurgöz completed her BS (1991), MS (1995), and PhD (2001) all in electrical engineering at the Istanbul Technical University, Turkey. She is interested in Heat Transfer, Numerical Methods, Design of Transformer and Electrical Machines. She is currently assistant professor of electrical engineering at Istanbul Technical University.